

Vibrational heat capacity of the carbon nanotubes in the low and ultra-low temperature region

M. V. Avramenko, I. Yu. Golushko, S. B. Rochal

Faculty of Physics, Southern Federal University, 5 Zorge Street, 344090 Rostov-on-Don, Russia

We develop a continuous theory of low-frequency dynamics for single-walled carbon nanotubes (SWCNTs) weakly interacting with the environment. In the frame of the approach proposed we determine the dependence of SWCNTs specific heat in the low ($T < 40$ K) and ultra-low ($T < 2.5$ K) temperature ranges. We show that taking into account the interaction between SWCNT and medium leads to frequency shifts of SWCNT modes with mainly radial polarization. We derive that even weak interaction which does not significantly change the vibrational spectrum of SWCNT decreases theoretical ultra-low specific heat dramatically. The discovered peculiarity properly explains available experimental data in contrast to the preceding theoretical papers. The theory proposed can be the basis for studies of low-temperature heat capacity and phonon dynamics of many other single-walled and multi-walled tubular structures (boron nitride, transition metal dichalcogenides) which have emerged in the past decade.

I. Introduction

Since their discovery [1], carbon nanotubes (CNTs) have held the researches' attention because of high potential for various technological applications [2-4] due to their unique fundamental properties. Low temperature (LT) heat capacity is one of such outstanding characteristics, and its temperature dependence still has been a matter of argument. Unfortunately, there are only a few experimental papers presenting results of SWCNTs specific heat measurements. For the first time specific heat temperature dependences were obtained in the ranges $0.6 < T < 210$ K [5] and $2 < T < 300$ K [6]. Later, some experiments were carried out at ultra-low temperatures (ULT) and the obtained results differed significantly: by 2-4 times at $T < 3.5$ K and 0.2-0.4 times at $3.5 < T < 4.5$ K.

It is generally agreed that the main contribution to heat capacity of CNTs and their bundles is made by phonon modes even at ULT. The theory of CNTs vibrational heat capacity has been developing rapidly. Currently, the two groups of approaches to theoretical studies of CNTs vibrational heat capacity exist. The first one include the methods based on computational modeling of SWCNTs vibrational dynamics, in particular, force-constant models [9-12] and methods of molecular dynamics [13, 14]. Large number of atoms in CNTs leads to huge amount of computation. Besides, complex multiparticle interaction potentials are to be used in order to yield satisfactory results. The authors of theoretical papers [9, 11, 12-14] state that their results are in quite good quantitative agreement with experimental data [6, 7]. However, in [9] it is reported that specific heat temperature dependence T^x has two regimes: linear at LT, then quadratic. On the contrary, in [14] it is stated that T^x function is quadratic at LT and then linear. And model [11] predicts the existence of three regimes instead of two in the temperature range $0 < T < 100$ K: $x=1/2$ at ULT (approximately at 0.5-0.8 K), then $x=1$ at $T < 5$ K and $x > 1$ at $T > 5$ K. Slight adjustments to the results of [11] were made in [12] by specifying that $0.6 < x < 1$ in the second regime. The specific heat temperature dependence obtained in [12] is in good agreement with experimental data [6] only in the range $2 < T < 30$ K.

Another well-known group of methods for SWCNTs thermal characteristics calculation is based on different continuous models, which usually consider SWCNT as a thin cylindrical shell [15-17]. Since continuous approaches do not take into account the discrete atomic structure of SWCNTs and therefore do not describe high-frequency range of their vibrational spectrum, it is impossible to obtain high-temperature heat capacity by means of these models. However, LT heat capacity of SWCNTs is entirely determined by their low-frequency dynamics, which, in turn, is almost independent of SWCNTs discrete structure [15, 18]. Thus LT heat capacities calculated in the frame of discrete and continuous models should be the same. Nevertheless, specific heat temperature dependence obtained in [16] is almost linear and, as a result, meanly describes experimental data [6]. In the revised version [17] of theory [16] it is demonstrated that specific heat temperature dependence has two regimes: $x=1$ at LT and $x > 1$ at temperatures higher than 180-200 K.

Thus, up-to-date notions of SWCNTs LT heat capacity are quite contradictory and, obviously, that is due to disadvantages of the models describing SWCNTs vibrational dynamics. In the recently

published paper [18] low-frequency vibrational spectra of both single-walled and double-walled CNTs were successfully described in the frame of new continuous theory of two-dimensional membrane dynamics. Following the classical theory of elasticity [19], the preceding approaches related membrane topological elasticity to its macroscopic thickness. Such approximations are obviously incorrect for nanomembranes of one atom thickness (like graphene and SWCNTs) and, as it is shown below, lead to certain mistakes in describing low-frequency spectrum of SWCNTs. The theory [18] considers bending elasticity of membrane of one atom thickness as phenomenological characteristics and describes 2D membrane using only three independent elastic constants. The aim of this paper is theoretical study of SWCNTs heat capacity dependence at LT in the frame of approach [18]. The proposed theory shows better agreement with experimental data [5-8] than the preceding models.

The paper is organized as follows. The second section is devoted to the analysis of SWCNTs dynamics, both individual and surrounded by medium. In the third section we discuss LT heat capacity of SWCNTs and compare the results obtained with available experimental and theoretical data. The Appendix considers some existing continuous models, which describe the phonon dynamics of SWCNTs.

II. SWCNTs dynamics subject to the interaction with environment

In this section we recall some results of approach [18], which considers graphene and nanotubes as 2D membranes of no macroscopic thickness. So far it has been impossible to measure heat capacity of individual SWCNT, thus the papers [5-8] are devoted to experimental studies of specific heat of SWCNTs bundles. Obviously, in this case CNTs cannot be considered as individual ones, and environment makes simple homogeneous contribution to the forces restoring nanotubes to their equilibrium state. Let us recall that individual SWCNT has four Goldstone degrees of freedom: rotation around its axis, translation as a whole along the tube axis and doubly degenerate translation as a whole in the direction normal to the axis. For individual SWCNTs comprising a system these degrees of freedom stop being of Goldstone type since neighboring nanotubes prevent free motion of each other. Thus in the system under consideration frequencies of all SWCNTs modes cannot vanish at $k \rightarrow 0$.

Let us note that elastic terms corresponding to restoring forces for translation and rotation of SWCNT as a whole should be significantly smaller (at least, one order less) than the term describing radial restoring force. Therefore we map out tangential and rotational restoring forces and write free energy density of 2D membrane in the following simplest form:

$$g = \frac{\lambda}{2} (\varepsilon_{ii})^2 + \mu \varepsilon_{ij}^2 + K(\Delta H)^2 + \frac{C}{2} u_r^2, \quad (1)$$

where λ and μ are 2D analogs of Lamé coefficients, K is topological bending rigidity, $\Delta H = H - H_0$ with H and H_0 standing for total and spontaneous mean curvatures of the surface, C is pinning coefficient describing the interaction between SWCNT and environment, ε_{ij} is a 2D strain tensor which generally depends on H_0 and 3D displacement field $\mathbf{u} = (u_r, u_\varphi, u_z)$ of membrane. The latter in cylindrical coordinates depends on the angle φ and the variable z , which measures the distance along the cylinder axis. The curvature deviation linearized with respect to the field \mathbf{u} and its derivatives reads $\Delta H = -(\Delta_s u_r)/(2R^2)$, where $\Delta_s = 1 + \partial_\varphi^2 + R^2 \partial_z^2$.

Equations of motion for the 2D membrane are obtained by variation of the functional:

$$A = \int (g(\mathbf{u}) - \rho \dot{\mathbf{u}}^2 / 2) dS dt, \quad (2)$$

where t is time, dS is the membrane area element, and ρ is the surface mass density. To derive the motion equations we substitute $dS = R dz d\varphi$, ΔH , and ε_{ij} in Eq. (2) and calculate the variation. The resulting equations have the following form:

$$\begin{aligned}
\ddot{u}_r \rho R &= -CRu_r - (\lambda + 2\mu) \left(\frac{u_r}{R} + \frac{\partial u_\phi}{R \partial \phi} \right) - \lambda \frac{\partial u_z}{\partial z} - K \frac{1}{R^3} \Delta_s^2 u_r, \\
\ddot{u}_\phi \rho R &= \frac{(\lambda + 2\mu)}{R} \left(\frac{\partial u_r}{\partial \phi} + \frac{\partial^2 u_\phi}{\partial \phi^2} \right) + (\lambda + \mu) \frac{\partial^2 u_z}{\partial \phi \partial z} + \mu R \frac{\partial^2 u_\phi}{\partial z^2}, \\
\ddot{u}_z \rho R &= (\lambda + \mu) \frac{\partial^2 u_\phi}{\partial \phi \partial z} + (\lambda + 2\mu) R \frac{\partial^2 u_z}{\partial z^2} + \lambda \frac{\partial u_r}{\partial z} + \mu \frac{\partial^2 u_z}{R \partial \phi^2}.
\end{aligned} \tag{3}$$

Substitution of $u_j = u_j^0 \exp(i(kz + n\phi - \omega t))$, where n is integer wave number, k is one-dimensional wave vector, ω stands for circular frequency, and $j = r, \phi, z$, yields dynamic matrix of the system (3). Vanishing of its determinant

$$\begin{bmatrix}
\frac{\lambda + 2\mu}{R} + \frac{KX^2}{R^3} + CR - R\rho\omega^2 & i \frac{(\lambda + 2\mu)n}{R} & ik\lambda \\
-i \frac{(\lambda + 2\mu)n}{R} & \frac{(\lambda + 2\mu)n^2}{R} + \mu k^2 R - \rho\omega^2 R & (\lambda + \mu)nk \\
-ik\lambda & (\lambda + \mu)nk & (\lambda + 2\mu)k^2 R + \frac{\mu n^2}{R} - R\rho\omega^2
\end{bmatrix}, \tag{4}$$

where $X = (R^2 k^2 + n^2 - 1)$, determines three real dispersion laws $\omega_j = \omega_j(k, n)$. Imaginary values of nondiagonal blocks in (4) reflect the $\pi/2$ phase shifts of the radial component with respect to the tangential ones.

Following [18] let us change the system of units to experimental one, where CNTs dimensions are measured in nm, the length of wave vector k is set in nm^{-1} , and solutions of $\det|\mathbf{M}|=0$ determine frequencies in cm^{-1} . We take the same estimations as in [18], in particular, $\lambda/\rho \approx 2400 \text{ cm}^{-2} \text{ nm}^2$, $\mu/\rho \approx 5200 \text{ cm}^{-2} \text{ nm}^2$, $K/\rho \approx 12.5 \text{ cm}^{-2} \text{ nm}^4$. The value of coefficient C depends on material of CNTs environment. In order to demonstrate the influence of radial pinning on vibrational spectrum of SWCNT we assume that $C/\rho \approx 4000 \text{ s}^{-2}$ (as an example) and plot dispersion curves for individual SWCNT (10, 10) and the same tube in medium (Fig. 1, solid black and dashed red curves, respectively).

Let us derive several particular solutions of equation $\det|\mathbf{M}|=0$ and obtain some analytical estimations for SWCNTs vibrational spectra. For $n=0$ and $k=0$ equality $M_{11}=0$ determines the dependence of RBM mode frequency on nanotube radius and pinning coefficient C . As $\lambda R^2 \gg K$ and $\mu R^2 \gg K$ [18] we exclude the term KX^2/R^3 and write the expression for RBM mode frequency in the following form:

$$\omega_{RBM} = \sqrt{\frac{\lambda + 2\mu}{R^2 \rho} + \frac{C}{\rho}}. \tag{5}$$

Let us note that if $C/\rho < 500 \text{ s}^{-2}$ then the shift of RBM mode frequency is less than experimentally registrable instrumental error, namely 1 cm^{-1} .

Taking into account relative infinitesimality of constant K it is possible to calculate the velocities of sound in SWCNTs. For individual nanotube at $n=0$ modes 2 and 3 (Fig. 1a) linearly vanish with $k \rightarrow 0$ and correspond to transversal rotational and longitudinal acoustic modes. The slope ratios of these dispersion curves determine the sound velocities in SWCNT. In order to obtain analytically expressions for velocities of longitudinal (V_{LA}) and rotational (V_{TA}) modes one should find the derivatives of corresponding solutions of $\det|\mathbf{M}|=0$ with respect to k assuming $k \rightarrow 0$, $n=0$, $C=0$ and using the estimations [18] introduced above. Thus we obtain

$$V_{LA} = \sqrt{\frac{4\mu(\lambda + \mu)}{\rho(\lambda + 2\mu)}}, \quad V_{TA} = \sqrt{\frac{\mu}{\rho}}. \tag{6}$$

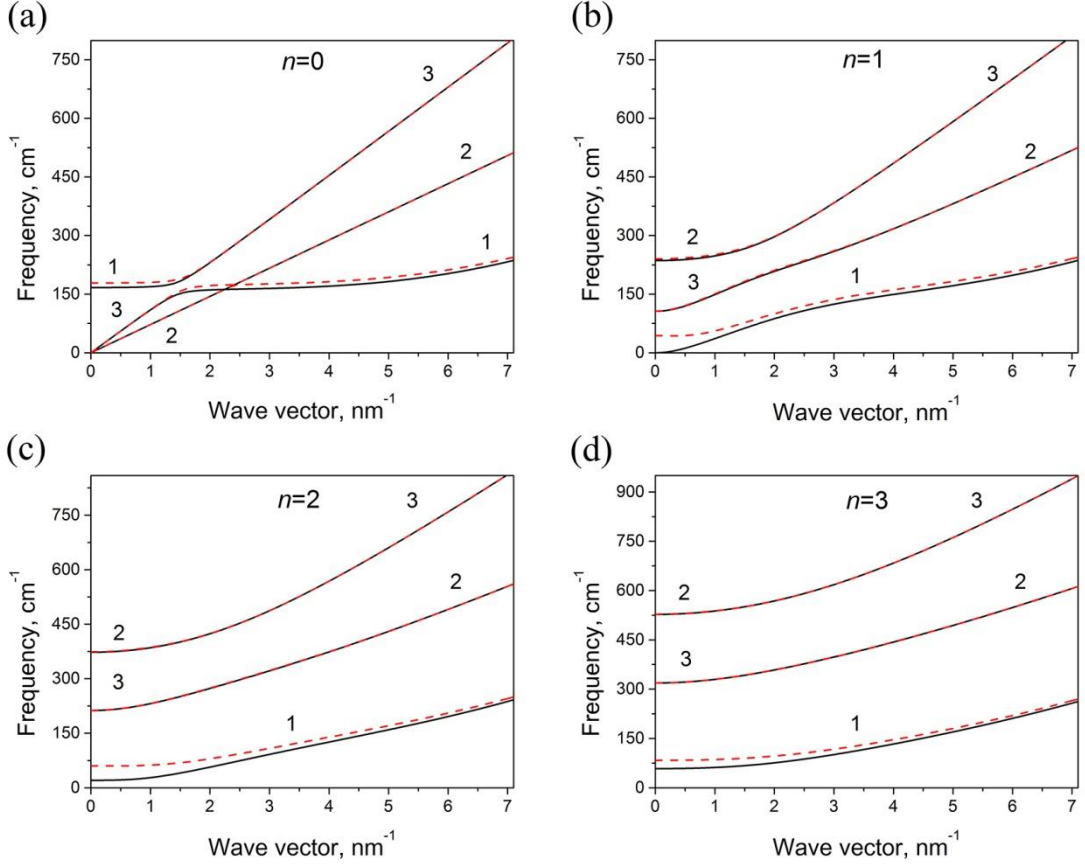


FIG.1. The dispersion curves for SWCNT (10, 10) and $n=0..3$ (panels a-d, respectively). Solid black curves correspond to individual nanotube and dashed red to one in a medium with $C/\rho \approx 4000 \text{ s}^2$. Let us note that all vibrations (except for some special cases) are characterized by mixed polarization since nanotube surface is curved. Modes with mainly radial, tangential and longitudinal polarizations are denoted with numbers 1, 2 and 3, respectively. Principal direction of polarization may depend on the wave vector length. The interaction between modes of the same symmetry leads to resonance and change of principal direction of polarization: it occurs at $k \approx 1-2 \text{ nm}^{-1}$ ($n=0$ and $n=1$), $k \approx 4 \text{ nm}^{-1}$ ($n=2$) and $k \approx 5 \text{ nm}^{-1}$ ($n=3$).

Let us note that mode 1 (Fig. 1b, $n=1$) determining the main contribution to ULT heat capacity (in the third section we discuss this question in detail) vanishes quadratically and its dispersion law at $k \rightarrow 0$ can be written as

$$\omega = \alpha k^2, \quad (7)$$

where $\alpha = \frac{V_{LA} R}{\sqrt{2}}$.

For the nanotube in medium with account for radial pinning the frequencies of modes which propagate with velocities determined by Eq. (6) do not virtually shift, but the frequency of the mode described by Eq. (7) at $k \rightarrow 0$ increases by approximately $\sqrt{\frac{C}{2\rho}}$ (Fig. 1b, $n=1$). Let us note that taking into account tangential and rotational pinning leads to analogous shifts at $k=0$ for corresponding acoustic modes. Similar shifts dramatically decrease ULT heat capacity, as it is described in detail in the next section.

Before we calculate heat capacity by means of obtained dispersion laws, let us clearly define the limitations of continuous model we use. Firstly, the phonons in SWCNTs subject to n and k can be characterized by the length of effective wave vector

$$k_{eff} = \sqrt{k^2 + \left(\frac{n}{R}\right)^2}. \quad (8)$$

The length (8), in turn, determines the effective wave length $2\pi/k_{\text{eff}}$, which is to be several times longer than interatomic distance 0.142 nm in SWCNTs. Secondly, SWCNTs band structure is periodic with period $2\pi/a$ in reciprocal space. For the nanotube (10, 10) $2\pi/a = 25.5 \text{ nm}^{-1}$. It means that at $k > 12.25 \text{ nm}^{-1}$ all dispersion curves on Fig. 1 should go down. Thus for the SWCNT under consideration the continuous model gives accurate results for k less than $6-7 \text{ nm}^{-1}$. In this case such restriction is more severe than the one we can get from Eq. (8). According to the latter, we derive that the maximum value for n_{lim} is 5. The obtained limitations to our continuous theory also constrain temperature range of continuous models applicability.

III. Discussion of SWCNTs low-temperature heat capacity and conclusions

In order to estimate temperature range of applicability we assume that modes with frequencies which do not satisfy the condition

$$\frac{h\nu}{k_B} \leq 9T \quad (9)$$

make negligibly small contribution to heat capacity. In Eq. (9) h is Planck constant, k_B stands for Boltzmann constant. The frequency of the lowest-energy mode (denoted as 1 on the Fig. 1b) at wave vector length corresponding to the applicability limit of continuous theory is approximately 200 cm^{-1} . At temperatures less than 37 K this mode does not virtually excite as all the modes of higher frequencies. It is precisely this fact that determines the upper limit of the applicability range of our model as 37 K.

Now let us recall some general information on SWCNTs vibrational spectrum, which is determined by the nanotube symmetry. The factor group of SWCNTs with respect to translational subgroup is D_N or D_{Nh} , where N is even integer equal to the number of carbon hexagons contained within the nanotube unit cell [20]. For any SWCNT modes with particular wave vector k are indexed by integers $n = -N/2 + 1, -N/2 + 2 \dots N/2$. Since the determinant (4) is quadratic in n and k , the modes of the same absolute values of n and k are equivalent to each other. Thus the modes with nonzero n and k are fourfold degenerate. Besides, for every n and k there are $2 \times 3 = 6$ vibrational modes, where multiplier 2 corresponds to the number of atoms per graphene unit cell, and 3 stands for three possible polarizations of mode [21].

Let us denote the length of SWCNT as L and its period as a . Thus the number of SWCNT atoms is given by $2NL/a$ and number of degrees of freedom is $6NL/a$. If the density of modes of particular type (for every n) is denoted as δ then $6N\delta \frac{2\pi}{a} = 6N \frac{L}{a}$ and $\delta = \frac{L}{2\pi}$, since the number of normal vibrations should be equal to the one of degrees of freedom. Next, the energy U of a collection of oscillators of frequencies ν_k in thermal equilibrium is equal to $h\nu_k$, and the number of oscillators in the state with wave vector k is determined by Planck distribution [22]. Thus full vibrational energy of SWCNT can be written in the following form:

$$U = \frac{L}{2\pi} \sum_{n=-\frac{N}{2}+1}^{\frac{N}{2}} \sum_{j=1}^6 \int_{-\frac{\pi}{a}}^{\frac{\pi}{a}} \frac{h\nu_j(k,n)}{e^{\frac{h\nu_j(k,n)}{k_B T}} - 1} dk. \quad (10)$$

At low temperatures Eq. (10) can be simplified and expressed as:

$$U = \frac{L}{\pi} \sum_{n=-n_{\text{lim}}}^{n_{\text{lim}}} \sum_{j=1}^3 \int_0^{\infty} \frac{h\nu_j(k,n)}{e^{\frac{h\nu_j(k,n)}{k_B T}} - 1} dk, \quad (11)$$

where n_{lim} is the maximum number of oscillations obtained above.

By differentiating Eq. (11) with respect to T and numerically integrating the result with respect to k we determine the dependence of SWCNTs specific heat on temperature without account for radial

pinning (black squares) plotted on Fig. 2 in comparison with experimental data [6] in the range $2 < T < 37$ K (empty asterisks). By means of obtained theoretical curve experimental data is fitted with approximately constant and independent of temperature absolute error. In the LT range relative error of fitting takes a turn for the worse since specific heat decreases itself. Taking into account radial interaction between SWCNT and environment allows us to improve fitting results significantly. Let us denote additional experimental data [7] in the ULT range as C_{Vi} and deviation of theoretical specific

heat from experimental one as ΔC_{Vi} . By minimization of meansquare relative error $\sum_i \left(\frac{\Delta C_{Vi}}{C_{Vi}} \right)^2$ we determine the pinning coefficient. The curve corresponding to specific heat dependence with account for obtained value $C/\rho=100 \text{ s}^{-2}$ is plotted on Fig. 2 with red squares.

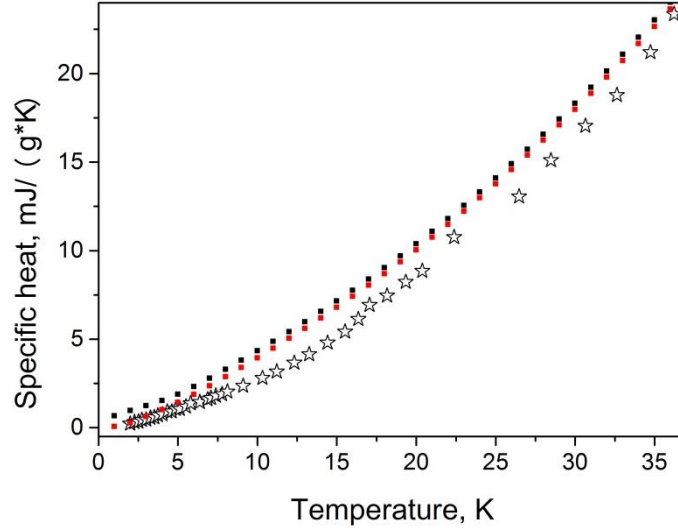


FIG. 2. Specific heat temperature dependences: theoretical ones with and without account for pinning (red and black squares, respectively) and experimental one (empty asterisks) obtained from a sample consisting mainly of SWCNT ropes [6].

In fact, all the models describing dynamics of individual SWCNTs are not suited for calculation of ULT heat capacity of SWCNTs bundle. In the ULT range ($T < 2$ K) theoretical specific heat is *by order of magnitude greater* than experimental one [7]. Let us prove it. Obviously, at $T \rightarrow 0$ the main contribution to heat capacity is made by vibrational mode of quadratic dispersion (7). The existence of this mode and its type of dispersion at $k \rightarrow 0$ are universally recognized by all dynamic theories starting from the paper [11]. Excluding the contribution from the rest of the modes we obtain the following lower bound for ULT heat capacity of SWCNTs:

$$C_V = \frac{3}{4} \zeta\left(\frac{3}{2}\right) \frac{Lk_B^2}{\sqrt{k_B \alpha h \pi}} \sqrt{T}, \quad (12)$$

where ζ – zeta function (its value at 3/2 is approximately 2.61), α is determined by SWCNT characteristics by means of Eq. (7), h – Planck constant. It appears that in discrete model [12] parameter α is approximately a half of the value obtained according to Eq. (7). Thus, at $T \rightarrow 0$ heat capacity in the frame of approach [12] significantly exceeds our data calculated without account for radial pinning (Fig. 2, black squares). Therefore, the paper [12] as the other ones [9-11, 13, 14] cannot explain experimental data in the ULT range, and their discussions of power x in the T^x law at $T < 2$ K are pointless.

As it was discussed above, taking into account the interaction between SWCNT and environment significantly improves the result of heat capacity fitting in the ULT range. Obviously, the obtained value $C/\rho=100 \text{ s}^{-2}$ is too weak to be experimentally registered by the frequency shift of RBM mode, but appears to be sufficient to decrease ULT heat capacity of SWCNTs dramatically. In addition to

Fig. 2, Fig. 3 shows experimental data [7] fitted by function $0.043T^{0.62}+0.035T^3$ [7] and theoretical specific heat calculated in the frame of our model at $C/\rho=100 \text{ s}^{-2}$ on a large scale.

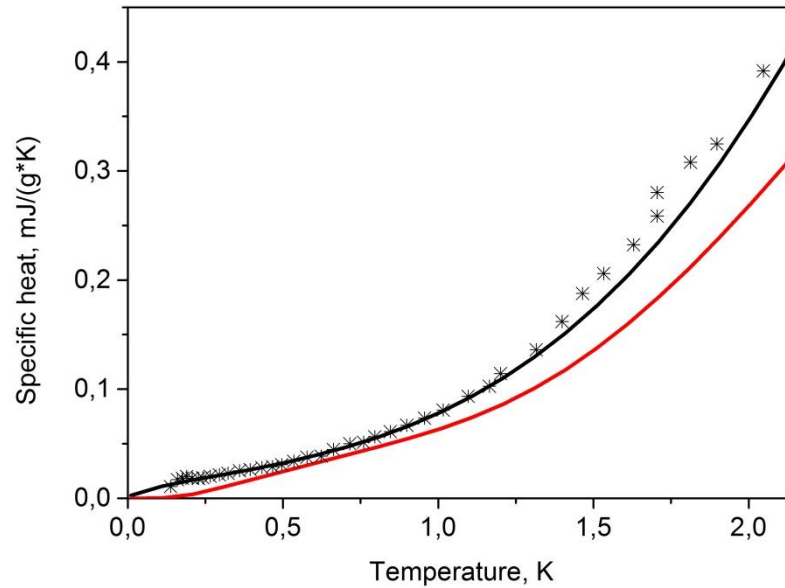


FIG. 3. Experimental data [7] fitted by function $0.043T^{0.62}+0.035T^3$ [7] (black curve) and theoretical specific heat calculated in the frame of our model at $C/\rho=100 \text{ s}^{-2}$ (red curve).

In conclusion, we developed a continuous theory of SWCNTs dynamics with account for their weak interaction with environment. The obtained results are applied to calculation of SWCNTs specific heat in the LT and ULT ranges. We ascertain that ULT heat capacity cannot be correctly derived without account for environmental influence on SWCNT. The interaction between SWCNTs and medium makes additional contribution to the forces restoring nanotubes to their equilibrium state and significantly changes the dispersion dependences type for the phonon modes with frequencies vanishing at $k \rightarrow 0$ in individual SWCNT. Taking into account radial and tangential interaction between SWCNT and environment results in nonzero frequencies of these modes even at $k=0$. Radial interaction with medium appears to be more significant than tangential one and therefore is discussed in this paper in detail. We demonstrate that even weak radial interaction between SWCNT and environment leads to a sharp fall in phonon density of states at $\omega \rightarrow 0$ and in heat capacity at $T \rightarrow 0$. As far as we know the approach proposed is the only one which results in theoretical specific heat dependence being in quantitative agreement with experimental data in the ULT range ($T < 2 \text{ K}$). Unfortunately, only two papers [7, 8] present results of measurements of ULT specific heat, and the dependences obtained differ significantly. That probably can be explained not only by inaccuracy of experiments but also by difference in pinning coefficient of the systems under consideration. Thus the proposed theory can be refined on taking into account tangential interaction between SWCNTs and medium if new experimental data emerge.

It is possible that effective interaction between SWCNT and environment grows with temperature. If it is ascertained in future, then, on the one hand, this fact will improve the agreement between theoretical data and experimental one in the range $2 < T < 40 \text{ K}$. On the other hand, the proposed theory or its modification can be applied to providing an explanation for the shift of RBM mode frequency observed in [23]. And, last but not least, our theory can be explored to study LT specific heat of multi-walled CNTs and many other tubular structures (boron nitride, transition metal dichalcogenides) emerged in the past decade.

References

- [1] S. Iijima, *Nature* **354**, 56–58 (1991).
- [2] R. Saito, G. Dresselhaus and M.S. Dresselhaus, *Physical Properties of Carbon Nanotubes* (Imperial College Press, London, 1998).

- [3] S. Reich, C. Thomsen and P. Ordejon, *Elastic Properties and Pressure-induced Phase Transitions of Single-walled Carbon Nanotubes*, Vol. **235** (Wiley Online Library, 2003).
- [4] A. Jorio, M.S. Dresselhaus and G. Dresselhaus, *Carbon Nanotubes: Advanced Topics in the Synthesis, Structure, Properties and Applications*, Vol. **111** (Springer, Berlin, 2008).
- [5] A. Mizel *et al.*, Physical Review B **60**, 3264-7 (1999).
- [6] J. Hone, B. Batlogg, Z. Benes, A. T. Johnson and J. E. Fischer, Science **289**, 1730-3 (2000).
- [7] J. C. Lasjaunias, K. Biljaković, Z. Benes, J. E. Fischer, and P. Monceau, Physical Review B **65**, 113409-4 (2002).
- [8] B. Xiang, C.B. Tsai, C.J. Lee, D.P. Yu, Y.Y. Chen, Solid State Communications **138**, 516–520 (2006).
- [9] E. Dobardžić, I. Milošević, B. Nikolić, T. Vuković, and M. Damnjanović, Physical Review B **68**, 045408-9 (2003).
- [10] J. X. Cao, X. H. Yan, Y. Xiao, Y. Tang, and J. W. Ding, Physical Review B **67**, 045413-6 (2003).
- [11] V. N. Popov, Carbon **42**, 991-995 (2004).
- [12] J. Zimmermann, P. Pavone, and G. Cuniberti, Physical Review B **78**, 045410-13 (2008).
- [13] Michael C H Wu and Jang-Yu Hsu, Nanotechnology **20**, 145401-6, (2009).
- [14] Chunyu Li and Tsu-Wei Chou, Physical Review B **71**, 075409-6 (2005).
- [15] S. S. Savinskiĭ and V. A. Petrovskiĭ, Physics of the Solid State **44**, No. 9, 1802–1807 (2002).
- [16] S. Zhang, M. Xia, S. Zhao, T. Xu and E. Zhang, Physical Review B **68**, 075415-7 (2003).
- [17] S.P. Hepplestone, A.M. Ciavarella, C. Janke, G.P. Srivastava, Surface Science **600**, 3633–3636, (2006).
- [18] S. B. Rochal, V. L. Lorman and Yu. I. Yuzyuk, Physical Review B **88**, 235435-6 (2013).
- [19] L. D. Landau and E. M. Lifshitz, *Theory of Elasticity* (Addison-Wesley, Reading, MA, 1959).
- [20] O. E. Alon, Phys. Rev. B **63**, 201403 (2001).
- [21] M. V. Avramenko, S. B. Rochal, and Yu. I. Yuzyuk, Phys. Rev. B **87**, 035407 (2013).
- [22] Ch. Kittel, *Introduction to Solid State Physics* (Wiley, USA, 2005).
- [23] R. Saito, M. Hofmann, G. Dresselhaus, A. Jorio, and M. S. Dresselhaus, Advances in Physics **60** (3), 413–550 (2011).